

## **MRI/TRUS Fusion for Prostate Biopsy: Early Results and Clinical Feasibility**

**R. Narayanan<sup>1</sup>, J. Kurhanewicz<sup>2</sup>, K. Shinohara<sup>2</sup>, D. Crawford<sup>3</sup>, A. Barqawi<sup>3</sup>, A. Simoneau<sup>4</sup>, and J. Suri<sup>1</sup>**

<sup>1</sup>Engineering, Eigen Inc., Grass Valley, California, United States, <sup>2</sup>University of California, San Francisco, California, United States, <sup>3</sup>University of Colorado, Denver, Colorado, United States, <sup>4</sup>University of California, Irvine, California, United States

### **Abstract**

Prostate cancer is multifocal and lesions are not distributed uniformly within the gland, and up to 40% of cancers are isoechoic. Magnetic resonance imaging (MRI) is being increasingly used in the assessment of prostate cancer. The excellent soft tissue contrast and easily discernible zones within the prostate provides high sensitivity to cancers.  $T_2$ -weighted imaging using an endorectal coil combined with a pelvic phased-array coil has been shown to provide high resolution images of the prostate, while coregistered MRSI has been shown to have improved specificity. A key challenge in using preoperative MRI and other emerging functional modalities for **prostate biopsy** in combination with transrectal ultrasound (TRUS) is the registration of these datasets. During an MRI exam the gland is pushed in the anterior direction against the pubic bone due to inflation of the rectal probe. Additional shape changes due to patient motion, or drugs can induce further differences in glandular shape between preoperative MRI and ultrasound during biopsy. In the proposed work, we model the deformation relating MRI and ultrasound nonlinearly so as to enable analysis of MRI in conjunction with ultrasound (color blended or side-by-side) to enable the planning of biopsy targets visually using multimodality information. To the best of the author's knowledge this is the first time MRI and TRUS volumes of the prostate were registered using a nonlinear deformation model.

### **Introduction**

$T_2$ -weighted imaging with endorectal coil provides high sensitivity to prostate cancers which are typically seen as locations with decreased signal intensity relative to neighboring structures. Currently transrectal ultrasound imaging is the most prevalent modality used for detection of cancers during biopsy. Reconstruction of a series of 2D ultrasound images to 3D is becoming popular. The combination of 3D images from MRI and ultrasound can help significantly improve analysis of data (e.g. many cancers may be isoechoic in TRUS). The proposed work is motivated by the need to model accurately nonlinear deformation between the two modalities, while at the same time fast in order to be clinically useful. Speed optimizations are achieved via the use of a graphics processing unit (GPU). We present early results to show the clinical feasibility of such an approach needing further validation on real subjects.

### **Method**

After the 3D transrectal ultrasound is acquired, a discrete dynamic contour based semiautomatic segmentation<sup>1</sup> method provides a triangulated surface description of the gland. A similar procedure is adopted for the  $T_2$ -weighted MRI image also. Registration between the 3D MRI and TRUS volumes were carried out in three steps: (1) Global surface alignment, (2) Deformable surface registration and (3) Elastically warping MRI to TRUS. In the first step, the surface from MRI ( $S_{MRI}$ ) was iteratively globally aligned to the TRUS surface ( $S_{TRUS}$ ) using an extended weighted Procrustes analysis<sup>2</sup>. Vertices that are not in alignment with corresponding vertices are weighted higher in estimating the global rotation and translation parameters. The result of this alignment was a rigidly transformed surface ( $S'_{MRI}$ ). After global alignment the tentative surface  $S'_{MRI}$  and  $S_{TRUS}$  are nonlinearly registered using an adaptive focus deformable model (AFDM)<sup>3</sup> to result in  $S''_{MRI}$ . A correspondence is thus established between the vertices of the original MRI surface and newly estimated surface  $S''_{MRI}$ . Finally the MRI volume is elastically warped<sup>4</sup> using these boundary conditions to register with TRUS.

### **Results and Conclusions**

An experiment on a two model 053 end-fire phantoms (CIRS, Norfolk, Virginia) made from Zerdine with 6 and 12 glass beads embedded were used. A 3D TRUS scan was acquired from a Philips HDI-3000 and a Terason t3000 for the 6 and 12 bead phantoms respectively. Prior to the MRI scan, an endorectal probe was inserted and inflated to 50 cc and 70 cc respectively. The glass beads were manually identified from both modalities. Registration is validated using two multimodality phantoms with 6- and 12-glass beads embedded that serve as fiducials. Registration between MRI (with endorectal balloon volume of 70 cc) and ultrasound volumes yielded average fiducial registration error of **3.58 mm** ( $\sigma = 0.82$  mm) and **3.16 mm** ( $\sigma = 1.39$  mm) respectively for 6 and 12 beads. Prior to registration, these errors were 24.9392 mm ( $\sigma = 1.14$  mm) and 10.76 mm ( $\sigma = 2.88$  mm) respectively. The algorithm was completely parallelized using compute unified device architecture (nVidia, Santa Clara, California) running on a GTX 280 GPU. The time taken to run registration was found to be approximately 13 seconds. Efforts are currently on to further speed up these algorithms without compromising registration accuracy. Fig. 1 shows a representative MRI slice warped to match the ultrasound surface. Table 1 summarizes the protocols and registration error measures computed at fiducials. Registration errors are comparable to predicate techniques. Extensive validation on more phantoms and real patients need to be performed to further validate our reported errors.

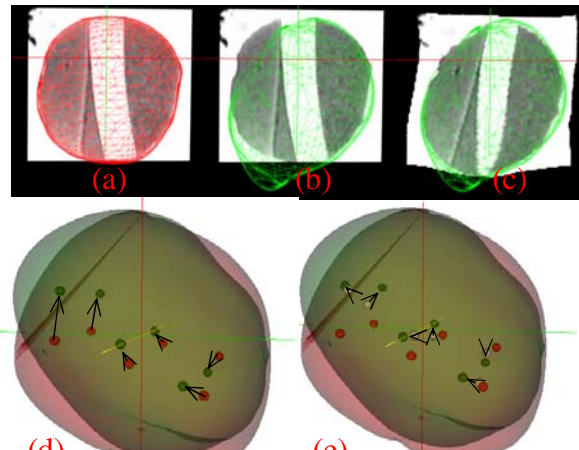


**Fig 1.** (a)  $S_{MRI}$  overlaid on MRI slice, (b)  $S_{TRUS}$  overlaid on the same MRI slice showing misalignment and (c) MRI slice warped to align with  $S_{TRUS}$  after registration. Correspondence between beads for 6 bead phantom (red for MRI, green for TRUS, and white for displaced beads from MRI after registration to TRUS) before and after registration are shown in (d) and (e).  $S_{MRI}$  is red, and  $S_{TRUS}$  is green. Arrows show distance between corresponding beads. Shorter arrows in (e) show improved bead correspondence after registration.

	<b>6 Bead Phantom</b>	<b>12 Bead Phantom</b>
<b>3D TRUS</b>	Philips HDI-3000	Terason t3000
<b>MRI</b>	Thin-section high-spatial resolution $T_2$ fast spin-echo (70 cc endorectal balloon)	
<b>Error <math>\mu(\sigma)</math> Before (mm)</b>	24.93 (1.14)	10.76 (2.88)
<b>Error <math>\mu(\sigma)</math> After (mm)</b>	<b>3.58 (0.82)</b>	<b>3.16 (1.39)</b>

**Table 1.** Results from 6 and 12 bead

### **References**

- [1] H. M. Ladak, F. Mao, Y. Wang, D. B. Downey, D. A. Steinman, and A. Fenster.,Prostate boundary segmentation from 2D ultrasound images. *Engg. In Medicine and Biology Society, Proc of 22<sup>nd</sup> Annual Int. Conf. of IEEE* 4, pp. 3188-3191, 2000.
- [2] C. Goodall. Procrustes methods in the statistical analysis of shape. *Journal of the Royal Statistical Society* 53, pp. 285-339, 1991.
- [3] D. G. Shen, E. Herskovits and C. Davatzikos. An adaptive focus statistical shape model for segmentation and shape modeling of 3D brain structures. *Engg. In Medicine and Biology Society, Proc of the 22<sup>nd</sup> Annual Int. Conf. of IEEE* 4, pp. 3188-2191, 2000.
- [4] C. Davatzikos. Spatial transformation and registration of brain images using elastically deformable models. *CVIU* 66(2), pp. 207-222, 1997.